

A&A manuscript no.
(will be inserted by hand later)

Your thesaurus codes are:
11.1.2,11.5.1,11.10.1,11.14.1

The HST snapshot survey of the B2 sample of low luminosity radio-galaxies: a picture gallery [★]

A. Capetti¹, H.R. de Ruiter^{2,3}, R. Fanti^{4,3}, R. Morganti⁵, P. Parma³, and M.-H. Ulrich⁶

¹ Osservatorio Astronomico di Torino, Strada Osservatorio 25, I-10025 Pino Torinese, Italy

² Osservatorio Astronomico di Bologna, Via Ranzani, 1, I-40127 Italy

³ Istituto di Radioastronomia, Via Gobetti 101, I-40129, Bologna, Italy

⁴ Dipartimento di Fisica dell'Università di Bologna, Via Irnerio 46, I-40126 Bologna, Italy

⁵ Netherlands Foundation for Research in Astronomy, Postbus 2, NL-7990 AA, Dwingeloo, The Netherlands

⁶ European Southern Observatory, Karl-Schwarzschild-Strasse 2, D-85748, Garching, Germany

Received 31 May 2000; accepted 31 August 2000

Abstract. A Hubble Space Telescope snapshot survey of the B2 sample of low luminosity radio galaxies has, at present, produced V and I images of 41 objects. Together with 16 images of B2 sources taken from the HST archive, there are now high resolution optical data for $\sim 57\%$ of the sample. All host galaxies are luminous ellipticals, except one which is a spiral galaxy, while another one turns out to be a misidentification.

We present an album of the images of the B2 radio galaxies observed so far, and give a brief description of the optical morphology of the galaxies. Dust features (in the form of disks, lanes or irregular patches) are seen in most of the galaxies of the sample, $\sim 58\%$. Compact optical cores are also very common (18/57). A preliminary analysis has revealed the presence of an optical jet in three objects, indicating they can be detected in a sizeable percentage in these low luminosity radio sources. Brightness profiles of dust-free galaxies are well represented by a Nuker law and all shows the existence of a resolved shallow cusp.

Key words: Galaxies: active; Galaxies: elliptical and lenticular, cD; Galaxies: jets; Galaxies: nuclei

1. INTRODUCTION

In the past few years, Hubble Space Telescope (HST) imaging of radiogalaxies has provided very valuable information on the optical structure of these sources. In particular, the HST/WFPC2 snapshot survey of the 3CR sample produced a large and uniform database of images

essential for a statistical analysis of their host galaxies (Martel et al. 1999, De Koff et al. 1996).

These studies revealed the presence of new and interesting features, some of them almost exclusively associated to low luminosity FR I radio-galaxies.

For example, HST observations have shown the presence of dust in a large fraction of radio galaxies which, however, takes the form of circum-nuclear disks (Jaffe et al. 1993; De Koff et al. 1996; De Juan et al. 1996, Verdoes Klein et al. 1999) only in FR I sources. These structures have been naturally identified with the reservoir of material which will ultimately accrete into the central black hole and might provide a direct approach to measure key parameters such as the accretion rate and the black hole mass in AGNs. Although the precise relationship between the symmetry axis of these disks and that of the sub-parsec scale structure is not yet fully established, they can represent useful indicators for the orientation of the central engine (Capetti & Celotti 1999). Several new optical jets have also been found in the HST images (e.g. Sparks et al. 1995, Baum et al. 1997, Martel et al. 1998): according to Martel et al. (1999) they are seen in $\sim 13\%$ of nearby ($z < 0.1$) 3CR radio galaxies and, with the only exception of 3C 273, all are found in FR I radio-galaxies.

FR I sources also represent an essential ingredient in the Unified Schemes of radio-loud AGNs as the mis-oriented counter part of BL Lac objects (see Urry & Padovani 1995 for a review). Indeed, recent radio studies have provided strong evidence in favour of relativistic beaming in their jets (Laing et al. 1999). Host galaxies of BL Lacs have been studied with the HST by Urry et al. (1999), and a similar analysis of galaxies hosting FR I sources should clarify if there is continuity in the properties of the respective nuclear regions, i.e. if any differences are due solely to orientation effects. Furthermore, Chiantera, Capetti & Celotti (1999) have shown that the nuclear sources commonly found in FR I might represent the optical counter part of the synchrotron radio cores.

Send offprint requests to: capetti@to.astro.it

[★] Based on observations with the NASA/ESA Hubble Space Telescope, obtained at the Space Telescope Science Institute, which is operated by AURA, Inc., under NASA contract NAS 5-26555 and by STScI grant GO-3594.01-91A

This opens the possibility of testing the unified models by directly comparing the anisotropic optical jet emission in BL Lac and FR I.

As many of the most extensively studied FR I radio galaxies are part of the B2 sample of low luminosity radio galaxies (Fanti et al. 1987), this prompted us to perform a complete, high resolution optical study of these ~ 100 sources. The radio characteristics of the B2 sample are different and in some sense complementary to those of the 3CR already studied with HST and they can fill the gap between the "radio quiet & normal" and the "radio loud" ellipticals.

A statistical study of such a large sample of low luminosity radio galaxies will enable us to establish how frequently we can detect optical jets, optical nuclear sources, circum-nuclear dusty disks and dust lanes and what is their relationship with the radio properties. Combining the HST observations of the B2 sample with those already existing of the complementary 3CR radio galaxies and BL Lac objects it will therefore be possible to find the similarities and differences of the optical nuclear properties as a function of radio power and morphological type of the parent optical objects. Particularly relevant will be, in this respect, the comparison of the optical brightness distribution of these samples of active sources with non active galaxies.

The organization of this paper is as follows; in Sect. 2 we briefly describe the B2 sample and give some general information. In Sect. 3 the present status of the HST observations is discussed and some relevant data on the program are given. The results are presented in Sect. 4, in the form of images and notes on the individual sources. Finally, in Sect. 5 we give a brief summary and discuss future work planned for the B2 sample.

Throughout this paper we use a Hubble constant $H_0 = 100 \text{ km s}^{-1} \text{ Mpc}^{-1}$ and $q_0 = 0.5$.

2. THE SAMPLE

Here we give a short description of the properties of the B2 sample of low luminosity radio galaxies. It consists of ~ 100 elliptical galaxies¹ identified with B2 radio sources (Colla et al. 1975; Fanti et al. 1978). The sample is complete down to 0.25 Jy at 408 MHz and down to a limiting magnitude $m_v = 16.5$. Since the sample was selected at low radio frequency, it is largely unbiased for orientation. The sample spans the power range between 10^{22} and 10^{25} WHz^{-1} at 1.4 GHz with a pronounced peak around 10^{24} WHz^{-1} and therefore gives an excellent representation of the radio source types encountered below and around the break in the radio luminosity function.

The B2 sample has been extensively studied at radio wavelengths, especially since the 1980's (see Fanti et

al. 1987, Parma et al. 1987, De Ruiter et al. 1990, Morganti et al. 1997). Comparison with Einstein Satellite X-ray data was done by Morganti et al. (1988). A number of B2 radio galaxies were subsequently observed with ROSAT (Feretti et al. 1995, Massaglia et al. 1996, Trussoni et al. 1997). Optical work on the sample has somewhat lagged behind, but a complete broad band imaging survey of the B2 sample was carried out by Gonzalez-Serrano et al. (1993) and Gonzalez-Serrano & Carballo (2000), while narrow band H α images were obtained by Morganti et al. (1992). The IRAS properties of the sample were studied by Impey & Gregorini (1993).

3. OBSERVATIONS AND DATA REDUCTION

Up till the present HST imaging was done for 57 of the ~ 100 radio galaxies. In the course of our HST program observations were obtained for 41 B2 galaxies, while public archive data exist for 16 additional objects, usually because these sources are also part of the 3C catalog (see De Koff et al. 1996, Martel et al. 1999, Verdoes-Klein et al. 1999). The HST observations also confirmed that the B2 radio galaxy 1441+26 is a misidentification (see Sect. 4.1) as already suggested by Gonzalez-Serrano & Carballo (2000).

Our program observations were obtained between April 9th and September 1st 1999, using the Wide Field and Planetary Camera 2 (WFPC2).

The pixel size of the Planetary Camera, in which all targets are located, is $0''.0455$ and the 800×800 pixels cover a field of view of $36'' \times 36''$. Two broad band filters were used, namely F555W and F814W, which cover the spectral regions 4500-6500 Å and 7000-9500 Å respectively. Although their transmission curve does not match exactly those of standard filters we will usually refer to them as V and I filters. The data have been processed through the PODPS (Post Observation Data Processing System) pipeline for bias removal and flat fielding (Biretta et al. 1996).

One image was taken through each filter and the exposure time was always set to 300 s (with the exception of B2 2116+26, which was observed for 350 s in the V band, as I band images were already available in the archive).

In order to minimize the overhead time associated to the read-out of the camera and to improve the efficiency of the program, we preferred to obtain a single image for each color as this enables us, e.g., to study also the color distribution in the inner regions of the galaxies. Obviously, with this choice, the removal of cosmic rays cannot be performed following the standard approach.

We thus identified cosmic rays events based on the comparison between the V and I images: each pixel where the ratio of the two images differed by more than a factor of 1.5 from its average value over the target and at the same time exceeded a threshold of 10 counts, was flagged as cosmic ray. The region within an expansion radius of 1.5

¹ the number of galaxies constituting the sample has recently undergone some changes. The present definition of the sample will be discussed elsewhere

Table 1. Log of archival HST observations

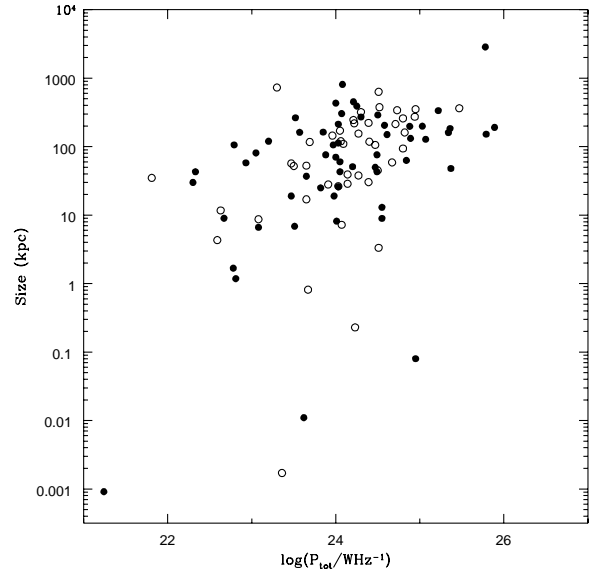
Name	Filter	t _{exp} (s)	Date	Prog. ID
0055+30	F814W	460	16/02/98	6673
	F555W	460	16/02/98	6673
0104+32	F702W	280	19/01/95	5476
0120+33	F555W	1600	13/07/97	6587
1003+35	F702W	280	19/10/94	5476
	F555W	600	12/06/96	6348
1217+29	F814W	460	07/05/94	5454
	F555W	1000	07/05/94	5454
1251+27	F702W	560	16/03/94	5476
	F555W	600	06/06/96	6348
1321+31	F814W	460	04/11/98	6673
	F555W	460	04/11/98	6673
1350+31	F702W	280	15/01/95	5476
1502+26	F702W	280	12/09/94	5476
1511+26	F702W	280	29/11/94	5476
1615+32	F702W	280	29/04/95	5476
	F555W	600	19/10/96	6348
1626+39	F702W	280	09/09/94	5476
1726+31	F702W	280	25/01/95	5476
1833+32	F702W	280	25/06/94	5476
2229+39	F702W	280	06/08/94	5476
2335+26	F702W	280	23/01/95	5476

pixel around each of them was replaced by interpolation of the nearest good pixels. Clearly this method is appropriate only for extended targets free of large gradients both in color and in intensity, such as are the objects studied for this project. A small number of faint cosmic rays and hot pixels are still present in the cleaned images. These were removed individually (with the IRAF task IMEDIT). The overall fraction of bad pixels is $\sim 1\%$: the images are not significantly affected by this process. Visual inspection of these final images indicates that the resulting images can be considered to be essentially free from strong cosmic rays that could have disturbed any further analysis (for example in the construction of brightness profiles).

The conversion from counts to the standard WFPC2 photometric system was derived using the header keyword PHOTFLAM of each filter which is accurate to within 2 % in the visible.

The archival images were reduced following the standard PODPS and cosmic rays removal procedure; the observing log for these sources is reported in Tab. 3.

The relevant data of the observed sources are given in Tab. 2: in columns 1 and 2 we give the radio source names (B2 and other), in column 3 the redshift, in columns 4 and 5 the total and core power at 1.4 GHz respectively, in columns 6 and 7 the largest angular size in arcsec and the largest linear size in kpc, the position angle of the main radio axis (in degrees) in column 8, where a “j” indicates the direction of the radio jets; finally the Fanaroff-Riley type is given in column 9. In a few cases no FR classification is possible (because of the lack of sufficiently high resolution observations), while for some other sources the

**Fig. 1.** Size vs radio power diagram for sources observed (filled circles) and not yet observed (empty circles) with HST

FR type is given as I-II; this classification concerns sources with a hybrid structure, i.e. in which both FR I and FR II characteristics are present.

While there is no bias in the selection of the sources of our program (they were chosen randomly as far as their radio and optical properties are concerned), a bias might have been introduced by the inclusion of the 16 archive sources. We thus compared various parameters of the observed sub-sample with those of the sources that were not observed by HST. This is illustrated in Figs. 1, 2 and 3; no significant differences emerged except for a small effect in redshift and total power. The median redshift and radio power of the two sub-samples are $z = 0.055^{+0.008}_{-0.011}$, $\log P_t = 24.05^{+0.07}_{-0.03}$ and $z = 0.067^{+0.005}_{-0.007}$, $\log P_t = 24.22^{+0.06}_{-0.03}$ respectively, thus only marginally different. We can then consider the sources observed with HST as well representative of the whole B2 sample.

4. RESULTS

In Fig. 4 we present the final broad band images of the innermost regions of all 57 B2 radio galaxies observed. In the left (right) bottom corner is indicated the size of the field of view in arcsec (kpc). Since the B2 sample contains ~ 100 objects this means that at present the HST observation are complete at the level of $\sim 57\%$.

A preliminary analysis of the HST images is presented in the notes on individual sources given below. In particular we checked for the presence of dust features, a compact optical core and an optical jet. The identification of optical cores is based on the procedure described in Chiaberge et al. (1999), i.e. a source brightness profile which, within

Table 2. Summary of the 1.4 GHz radio data of the sample.

B2 Name	Other Name	Redshift	$\log P_t$ (P in W/Hz)	$\log P_c$ (P in W/Hz)	l.a.s. arcsec	l.l.s. kpc	p.a. degr.	FR type
0034+25		0.0321	23.20	21.77	274	120	-87j	I
0055+26	4C26.03	0.0472	24.61	22.30	240	150	-40j	I
0055+30		0.0167	24.08	23.30	3450	811	-50	I
0104+32	3C 31	0.0169	24.21	22.63	1900	452	-20j	I
0116+31	4C31.04	0.0592	24.95	22.80	0.1	0.08	-80	
0120+33		0.0164	22.30	20.76	130	30	-80	I
0149+35		0.0160	22.33	21.54	191	43	65	I
0648+27		0.0409	23.62	22.92	0.02	0.011	-	
0708+32		0.0672	23.51	23.02	8	7	-5	
0722+30		0.0191	22.67	22.02	35	9	-85	I
0755+37		0.0413	24.49	23.59	138	76	-65	I
0908+37		0.1040	24.84	23.46	51	63	15	I-II
0915+32		0.0620	24.00	22.56	540	432	30	I
0924+30		0.0266	23.52	<20.5	720	264	60	I
1003+26		0.1165	24.01	22.10	6	8	10	
1003+35	3C236	0.0989	25.78	24.00	2400	2860	-60	II
1005+28		0.1476	24.25	22.60	240	391	-25	I-II
1101+38		0.0300	23.97	23.33	257	106	90	
1113+24		0.1021	23.65	<22.35	30	37	50	I
1204+34		0.0788	24.47	23.05	51	50	-50	II
1217+29		0.0021	21.24	21.22	0.03	0.001		
1251+27	3C277.3	0.0857	25.37	23.30	45	48	-22	II
1256+28		0.0224	23.05	21.03	260	81		I
1257+28		0.0239	23.08	20.69	20	7		I
1321+31		0.0161	23.85	21.77	720	163	-60	I
1322+36	4C36.24	0.0175	24.55	22.38	53	13	15	I
1339+26	4C26.41	0.0757	24.30	<22.5	285	271	30	I
1346+26	4C26.42	0.0633	24.55	23.37	11	9	25	I
1347+28		0.0724	24.05	22.27	47	43	50	I-II
1350+31	3C293	0.0452	25.03	23.34	331	199	90j	I-II
1357+28		0.0629	24.03	22.45	139	113	0j	I
1422+26		0.0370	24.00	22.24	140	70	-85	I
1430+25	4C25.46	0.0813	24.20	<21.9	50	51	20	I
1447+27		0.0306	22.78	22.51	4	2	27	
1450+28		0.1265	24.50	23.01	200	290	-60	I
1455+28	4C28.38	0.1411	25.22	<23.03	213	336	38	II
1457+29		0.1470	24.89	23.83	81	132	-25	I
1502+26	3C310	0.0540	25.36	23.40	260	184	-15	I
1511+26	3C315	0.1078	25.34	<24.3	125	160		I
1512+30		0.0931	23.82	21.00	22	25	-17	
1521+28	4C28.39	0.0825	24.58	23.50	200	205	-30j	I
1525+29		0.0653	23.98	22.10	23	19	30j	I
1527+30		0.1143	24.05	22.80	45	60	45j	I
1553+24		0.0426	23.57	23.01	285	162	-40j	I
1557+26		0.0442	22.81	<22.80	2	1	-	
1610+29		0.0313	22.93	<21.0	135	58	70	I
1613+27		0.0647	24.03	22.69	31	26	-37	I
1615+32	3C332	0.1520	25.79	23.43	91	152	15	II
1626+39	3C338	0.0303	24.49	23.16	103	43	90	I
1658+30A	4C30.31	0.0351	23.88	22.89	160	76	55	I-II
1726+31	3C357	0.1670	25.89	23.34	107	191	-70	II
1827+32		0.0659	24.07	23.08	360	304	75	I
1833+32	3C382	0.0578	25.07	23.85	170	128	50	II
2116+26		0.0164	22.79	22.08	457	106	-23j	I
2229+39	3C449	0.0181	24.03	22.11	840	213	10j	I
2236+35		0.0277	23.47	21.74	47	19	45j	I
2335+26	3C465	0.0301	24.88	23.22	480	198	-55j	I

5 pixels from the center, shows a FWHM consistent with the HST Point Spread Function ($\leq 0''.08$). As to the presence of optical jets, we just checked that after subtraction of a model galaxy, some emission was left at the location of the radio jet. We stress that a more detailed analysis will be carried out by us elsewhere. A summary of the optical data is given in Tab. 3, in which we give the names of the sources (B2 and other) in columns 1 and 2, the redshift in column 3; the presence of dust is indicated in column 4 as d (disk-like structure), l (dust lane, band or filament),

p (irregular patches); if possible we measure a position angle of the disk or band and the P.A. (in degrees from north through east) is given in column 5; the presence of unresolved optical cores and jets is indicated in columns 6 and 7.

4.1. Notes on the individual sources

0034+25: There is a prominent dust band in the center of this galaxy, likely a highly inclined dusty disk ori-

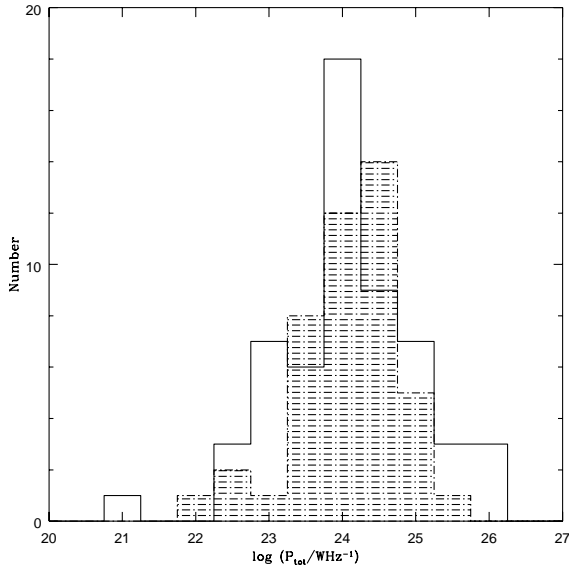


Fig. 2. Distribution of total power for sources observed and not yet observed (shaded) with HST

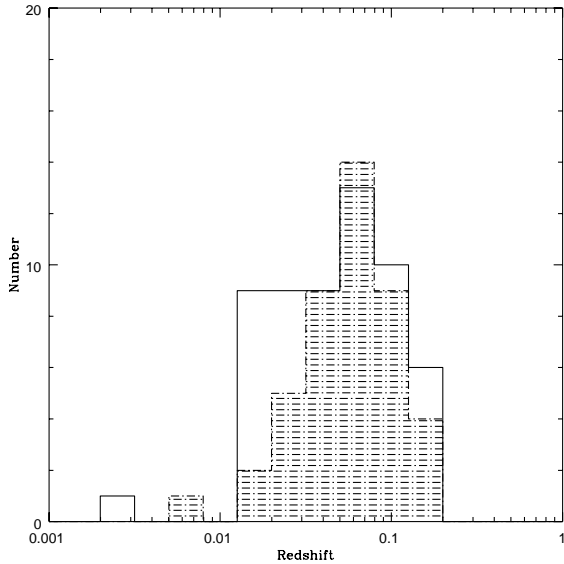


Fig. 3. Distribution of redshifts for sources observed and not yet observed (shaded) with HST

Table 3. Summary of optical data of the sample.

Name	Other Name	Redshift	Dust Morph.	P.A.	Core Opt.	Jet Opt.
0034+25	UGC00367	0.0321	d	160		
0055+26	NGC0326	0.0472				
0055+30	NGC0315	0.0167	d+p	40	yes	
0104+32	NGC0383	0.0169	d	40	yes	
0116+31		0.0592	l	25		
0120+33	NGC0507	0.0164				
0149+35	NGC0708	0.0160	l+p			
0648+27		0.0409	p			
0708+32		0.0672				
0722+30		0.0191	l			
0755+37	NGC2484	0.0413			yes	yes
0908+37		0.1040	d?	40	yes	
0915+32		0.0620	d			
0924+30		0.0266				
1003+26		0.1165				
1003+35		0.0989	l	50		
1005+28		0.1476	p			
1101+38	MRK 421	0.0300			yes	
1113+24		0.1021				
1204+34		0.0788				
1217+29		0.0021			yes	
1251+27	Coma A	0.0857	p		yes	
1256+28	NGC4869	0.0224	d?			
1257+28	NGC4874	0.0239				
1321+31	NGC5127	0.0161	l	45		
1322+36	NGC5141	0.0175	l	85		
1339+26	UGC08669	0.0757	l	0		
1346+26		0.0633	l	0	yes	
1347+28		0.0724	p			
1350+31	UGC08782	0.0452	l+p			
1357+28		0.0629	l	95		
1422+26		0.0370				
1430+25		0.0813				
1447+27		0.0306	l	145		
1450+28		0.1265				
1455+28		0.1411	l+p			
1457+29		0.1470	l	30		
1502+26		0.0540			yes	
1511+26		0.1078				
1512+30		0.0931	p			
1521+28		0.0825			yes	
1525+29	UGC09861	0.0653	l	25		
1527+30		0.1143	d?			
1553+24		0.0426			yes	yes
1557+26		0.0442				
1610+29	NGC6086	0.0313				
1613+27		0.0647	p			
1615+32		0.1520			yes	
1626+39	NGC6166	0.0303	p		yes	
1658+30A		0.0351				yes
1726+31		0.1670	l			
1827+32		0.0659				
1833+32		0.0578			yes	
2116+26	NGC7052	0.0164	d	65	yes	
2229+39	UGC12064	0.0181	l	165	yes	
2236+35	UGC12127	0.0277			yes	
2335+26	NGC7720	0.0301	d		yes	

ented along P.A. $\sim 160^\circ$. At larger radii, isophotes are very cuspy and oriented at the same position angle as the inner disk, which indicates the presence of a stellar disk coplanar with the inner one. The galaxy belongs to the Zw cluster 0034.4+2532.

0055+26 (NGC 326): This is a system of two galaxies, also referred to as a dumbbell galaxy. Only the galaxy hosting the radio source is shown. The two galaxies do not show any peculiarities. There is a third much fainter

object in the field. The galaxy belongs to a group with extended X-ray emission (Worrall et al. 1995)

0055+30 (NGC 315): A highly inclined, very regular circum-nuclear disk, is seen in absorption in this galaxy. It is oriented at P.A. $\sim 40^\circ$ and extends to $r \sim 350$ pc. At its center there is an unresolved nuclear source. Irregular dust patches are also present on the South side of the galaxy. See also Verdoes Kleijn et al. (1999).

0104+32 (NGC 383, 3C 31): An extended circum-nuclear dusty disk is seen at low inclination, with an unresolved nuclear component at its center. The disk diameter is $\approx 7''$ (2.5 kpc) along the major axis (P.A. $\sim 40^\circ$). The galaxy belongs to a chain of which it is the brightest member. See also Martel et al. (1999) and Verdoes Kleijn et al. (1999).

0116+31: An S-shaped dust lane bisects its nuclear region. Its inner P.A. is $\sim 25^\circ$. Conway (1996) detected a disk of HI in absorption which fully occults one of the minilobes and partially covers the other.

0120+33 (NGC 507): Brightest galaxy of the Zw cluster 0107+3212. The galaxy appears very regular and smooth.

0149+35 (NGC 708): A low brightness galaxy whose nuclear regions are crossed by an irregular dust lane and dust patches. It is the brightest galaxy of the cluster Abell 262.

0648+27: A galaxy with an irregular morphology, enhanced by the presence of dusty features. On its northern side there is a chain of knots, probably regions of star formation, parallel to the dusty filaments.

0708+32: The host galaxy does not exhibit any obvious peculiarities.

0722+30: The only source of the B2 sample associated with a spiral galaxy. It is a highly inclined galaxy which fills the PC field of view. Strong absorption is associated with its disk and a bulge-like component is also clearly visible. The radio emission originates from two symmetric jet-like features at an angle of 45° to the disk.

0755+37 (NGC 2484): The galaxy is characterized by a central unresolved nuclear source. After subtraction of a galaxy elliptical model the presence of a one-sided optical jet is revealed, cospatial with the SE brighter radio jet.

0908+37: This galaxy shows a point-like nucleus at the center of a highly elongated absorption feature, possibly an edge-on disk (P.A. $\sim 40^\circ$). A fainter companion galaxy (outside the image shown) is located $3.7''$ to the SW.

0915+32: A disk-like dust band surrounds its nuclear region.

0924+30: The host galaxy does not exhibit any obvious peculiarities.

1003+26: A very regular low brightness elliptical galaxy with no outstanding morphological features. The galaxy belongs to the cluster Abell 923.

1003+35 (3C 236): An off-centered dust lane crosses the galaxy to the SW, with $\approx 6''$ (2.5 kpc) extension. See also Martel et al. (1999).

1005+28: A diffuse and quite regular galaxy with no evident morphological peculiarities. A dust patch is visible.

1101+38: This source is associated with the BL Lac object Mrk 421. Not surprisingly it is dominated by its bright unresolved nucleus which produces strong diffrac-

tion spikes. Nonetheless a smooth elliptical host galaxy is clearly visible.

1113+24: A round smooth elliptical galaxy with a faint companion $\sim 3''$ to the north. The galaxy is the brightest of the Zw cluster 1113.0+2452.

1204+34: Dust patches produce a spiral structure, which is clearly visible in both bands. It extends out to at least $2''$ from a fully resolved nucleus. A secondary, again resolved, nucleus is found to the NE at a distance of $\approx 2''$. Both nuclei are embedded in a common elliptical halo, centered on the brighter one.

1217+29 (NGC 4278): This source is associated with the nearby galaxy NGC 4278. It shows a regular structure only slightly modified by diffuse dust absorption to its NW side. The nucleus is unresolved. The radio source is very compact, ≈ 1 pc (see, e.g., Schilizzi et al. 1983). The galaxy is known to have strong nuclear emission lines (Osterbrock 1960). It contains a large amount of neutral hydrogen (Raimond et al. 1981) rotating around an axis at -45° .

1251+27 (Coma A, 3C 277.3): In addition to a prominent unresolved nucleus, note also the filamentary structure located $\approx 7''$ to the SW. This corresponds to the radio knot K1 in van Breugel et al. (1985), detected also in emission lines. See also Martel et al. (1999).

1256+28 (NGC 4869): This galaxy presents a highly elongated absorption feature, possibly an edge on disk. It belongs to the Coma Cluster (Abell 1656).

1257+28 (NGC 4874): A very regular low brightness elliptical galaxy. It is one of the two dominant members of the Coma Cluster (Abell 1656).

1321+31 (NGC 5127): A dark lane covers the nucleus of this galaxy and extends out to a radius of $1''$, P.A. $\sim 45^\circ$. The galaxy belongs to the Zwicky cluster 1319.6+3135. See also Verdoes Kleijn et al. (1999).

1322+36 (NGC 5141): There is a wide dust band in the center of this galaxy, at P.A. $\sim 85^\circ$. See also Verdoes Kleijn et al. (1999).

1339+26: A small dark nuclear band (P.A. $\sim 0^\circ$) characterizes this otherwise very regular galaxy. The galaxy is the eastern of a double system and is the dominant member of the cluster Abell 1775.

1346+26: A low brightness galaxy with an unresolved nucleus and dust in the form of an irregular lane and patches (P.A. $\sim 0^\circ$). A sort of tail is seen to the SW towards a companion. It is the brightest galaxy (cD) of the cluster Abell 1795.

1347+28: A regular elliptical galaxy with irregular dusty features. It belongs to Abell 1800.

1350+31: A highly irregular galaxy, with two compact emission knots separated by a filamentary dust lane which extends to form a fan-like shape at larger radii. See also Martel et al. (1999). See Akujor et al. (1996) for a high resolution radio map showing a flat spectrum core with a two sided jet.

1357+28: A round elliptical galaxy with a small dust lane (P.A. $\sim 95^\circ$) bisecting the nuclear region.

1422+26: The host galaxy is very smooth with no outstanding morphological features. The bright central core is fully resolved.

1430+25: This elliptical galaxy does not exhibit any obvious peculiarities. An elongated nucleus has its major axis at P.A. $\sim 155^\circ$. The radio-structure is head-tail type, but no obvious cluster or group is visible.

1441+26: The target is a spiral galaxy. However, comparison of the radio and optical maps shows that this is not the host of the radio source. The correct identification is with a faint elliptical galaxy located at RA = 14:41:56.35, Dec = 26:14:05.0. As the magnitude of this galaxy is well below the optical selection threshold of the B2 sample, it must be considered a misidentification.

1447+27: Two off-center linear dust lanes run $0''.6$ and $1''.2$ respectively north-east of the nucleus (P.A. $\sim 145^\circ$) of this otherwise very regular galaxy.

1450+28: Elliptical galaxy with no outstanding features. In Abell 1984.

1455+28: The presence of hour-glass shaped dust absorption gives this galaxy a quite irregular appearance. The central knot is compact but completely resolved. Companion galaxy at $\approx 10''$.

1457+29: A wide dust lane (P.A. 30°) runs perpendicularly to the galaxy projected minor axis. The redshift of the galaxy has been measured recently by Gonzalez-Serrano & Carballo (2000); this value has been added in Tab. 2.

1502+26 (3C 310): A smooth elliptical galaxy with a central unresolved source. See Martel et al. (1999).

1511+26 (3C 315): This galaxy shows a very high nuclear ellipticity which contrasts with the typical roundness of the B2 host galaxies. The ellipticity decreases at larger radii but the central very elongated central structure clearly extends at larger radii, probably indicative of an edge-on stellar disk. The radio source has a very peculiar, two-banana shaped, radio-structure. See de Koff et al. (1996).

1512+30: The host galaxy does not show any outstanding morphological features, except for very faint elongated dust absorption at the center.

1521+28: A well defined unresolved nucleus is superposed on the smooth core of the galaxy.

1525+29: The double peaked nuclear structure is caused by dust absorption, which is extended in the direction P.A. $\sim 25^\circ$. The galaxy is the fainter of a pair in the cluster Abell 2079.

1527+30: The faint absorption from a possibly disk-like dust band is visible on the west side of this galaxy, extending to a radius of $0''.3$. Its central region is resolved. In Abell 2083.

1553+24: This galaxy exhibits a point-like nucleus and, after removal of an elliptical model for the galaxy

emission, a faint one-sided optical jet, cospatial with the NW brighter radio jet.

1557+26: A smooth and regular elliptical galaxy.

1610+29 (NGC 6086): This galaxy does not exhibit any obvious peculiarities. It is the brightest galaxy of the cluster Abell 2162.

1613+27: Very faint absorption features are seen to the SW on this otherwise regular galaxy.

1615+32 (3C 332): The emission of this source is dominated by its bright unresolved nucleus. A companion is seen to SW.

1626+39 (NGC 6166, 3C 338): Brightest galaxy of the cluster Abell 2199. An unresolved nucleus is superposed on the flat core of the galaxy. An arc-like dust feature extends from the nucleus to the W for $\approx 3''$. Two fainter elliptical companions are also present. (see Martel et al. 1999).

1658+30: Smooth galaxy with a central unresolved core. The subtraction of an elliptical galaxy model reveals the presence of a faint one-sided optical jet, cospatial with the radio jet.

1726+31 (3C 357): The central knot is well resolved. A dust lane is also present on its SW side.

1827+32: Round galaxy with a possible weak nucleus.

1833+32 (3C 382): This source is associated with the broad line radio galaxy 3C382. The nuclear emission dominates the optical emission but the underlying host galaxy is clearly seen in these images. See also Martel et al. (1999).

2116+26 (NGC 7052): A spectacular, highly inclined disk-like structure of dust (at P.A. $\sim 65^\circ$) surrounds the central source of this galaxy. See also Verdoes Kleijn et al. (1999). From the kinematics of the gas disk van der Marel & van den Bosch (1998) deduced the presence of a central black hole with a mass of $3 \times 10^8 M_\odot$.

2229+39 (3C 449): A wide band of absorption is located on the West side of this source, at P.A. $\sim 165^\circ$. See also Martel et al. (1999). Note also the prominent unresolved nuclear source.

2236+35: A faint nucleus, probably unresolved, is seen in this elliptical galaxy.

2335+26 (NGC 7720, 3C 465): It is the brightest galaxy in the cluster Abell 2634. An elliptical region of dust absorption is located around the bright unresolved nucleus of this galaxy. See also Martel et al. (1999).

4.2. Discussion

All B2 sources are hosted by bright elliptical galaxies, with the only exception of B2 0722+30, which is associated to a spiral galaxy. While this result might appear surprising, we must note that both the size (9 kpc) and the radio luminosity ($\log P_t = 22.67$) of this source place it at the lowest end of the range covered by the B2 sample. On the other hand these values are quite typical of radio-sources

associated to Seyfert galaxies (Nagar et al. 1999) which are indeed associated to spiral galaxies.

Brightness profiles of all elliptical host galaxies which are not severely affected by dust extinction can be successfully represented by a Nuker law (Lauer et al. 1995). In all cases we found evidence for a well resolved, shallow ($\gamma \leq 0.3$) central cusp, as expected given their range of absolute magnitudes, M_V from -20 to -23 .

In 18 of the 57 ($\sim 32\%$) B2 sources observed with the HST we found evidence for an unresolved nuclear source (see Tab. 3) down a magnitude level of $V = 23.5$. The detection rate is slightly lower than the percentage (between 43 and 54 %) found for 3C sources with $z < 0.1$ (Martel et al. 1999). This discrepancy can be accounted for noting that B2 sources have on average fainter radio cores than 3C sources (Giovannini et al. 1988) and that the optical emission in FR I nuclei strongly correlate with the radio core flux (Chiaberge et al. 1999). We thus expect that B2 galaxies harbour fainter optical cores which might be more difficult to detect against the galaxy background. Indeed the B2 sources in which we detected an optical core have higher radio core fluxes and more dominant cores than average.

Dust is frequently present in B2 sources: after visual inspection of the images we found that 33/57 (58 %) of them show dust features, either in the form of bands or disk-like structures, or more irregular patches. The percentage may be slightly higher than in 3C sources with $z < 0.1$, which have 37-48 % of sources with dust. Concerning the presence of dust features it does not appear that there is any difference between FR I and FR II objects: the FR I sources with dust are 19/35 (54 %), while the FR I-II and FR II with dust are 8/12 (66 %). Our data strengthen the findings by Martel et al. (1999) which found disk-like structures only associated to FR I type radio sources (see Tabs. 2 and 3). Indeed in the B2 sample, although dust is equally present in FR I and FR II sources, it is found to be ordered into disk-like structures in 9 FR Is while this behaviour is never found in FR IIs. However, the detection of dusty disks is almost exclusive of nearby ($z \lesssim 0.03$) galaxies. Within this distance there are only a handful of FR II in the 3C sample and none in the B2. This raises the question of the importance of the observational biases in our ability of finding such disks in FR II sources. Among the 18 sources with an optical core 9 also show the presence of dust, while no dust is detected in the remaining 9; a slightly higher rate of dust occurrence (24/39) is found among the sources without optical core. This suggests that extended dust structures might be hiding optical cores in a few cases. We find no connection between dust content and with largest radio linear size: the sources with dust have a median linear size of 94 ± 35 kpc, against 76 ± 30 for the sources without dust.

A first scrutiny of the B2 data indicates that detection of optical counter part of radio jet is not particularly rare. At present we have found three optical jets, in

B2 0755+37, B2 1553+24 and B2 1658+30A (see Tab. 3), but we do not exclude that a more refined analysis will produce a few more. Therefore optical jets in HST images of these low luminosity radio galaxies might be detected in a sizeable fraction of the sample, probably comparable with the 13 % found in the low redshift 3C sources. All optical jets are associated to strongly one-sided sources, of relatively small linear sizes and with prominent radio nuclei in agreement with the results by Sparks et al. (1995).

5. SUMMARY AND FUTURE WORK

We have presented HST/WFPC2 snapshot images in two bands (V and I) of 57 (out of a total of ~ 100) sources from the B2 sample of low luminosity radio-galaxies. One more object (1441+26), not shown in Fig. 4 has been found to be a mis-identification since the radio source appears to be associated with a background galaxy whose magnitude is below the optical selection threshold of the sample. Except for B2 0722+30, which is associated with a spiral galaxy, all sources are hosted by bright elliptical galaxies well fitted by Nuker laws, with shallow central cusps.

Most of the galaxies present a peculiar morphology. Almost 60 % show the presence of large scale dust structures which in 9 cases (all FR I radio sources) is distributed in well defined disks. In three sources we detected an optical synchrotron jet. The presence of central unresolved sources is revealed in 18 galaxies.

The present work is only a first presentation of the HST snapshot survey of B2 radio galaxies. While awaiting completion of the survey, more detailed studies will be presented in the near future. In particular an analysis of the brightness profiles will be given with a comparison of samples of powerful radio galaxies as well as non active galaxies, together with an exhaustive search for optical jets. Because of the relatively large number of objects it may be possible to study the orientation of optical features, such as dust-disks and -lanes, as compared to the main radio axes. Also the statistics of unresolved cores will be discussed in the framework of Unified Models, and in this respect a comparison with the sample of BL Lac objects that has already been observed with the HST will become crucial.

Acknowledgements. This research has made use of the NASA/IPAC Extragalactic Database (NED) which is operated by the Jet Propulsion Laboratory, California Institute of Technology, under contract with the National Aeronautics and Space Administration.

References

- Akujor Chidi, E., Leahy, J.P., Garrington, S.T., Sanghera, H., Spencer, R.E., Schilizzi, R.T., 1996, MNRAS 278, 1
- Baum, S.A., O'Dea, C.P., Giovannini, G., et al., 1997, ApJ, 483, 178

- Biretta, J.A., Burrow, C., Holtzman, J., et al., 1996, *Wide Field and Planetary Camera 2 Instrument Handbook*, ed. J.A. Biretta (Baltimore: STScI)
- Capetti, A., Celotti, A., 1999, *MNRAS*, 304, 434
- Chiaberge, M., Capetti, A., Celotti, A., 1999, *A&A*, 349, 77
- Colla, G., Fanti, C., Fanti, R., et al., 1975, *A&AS*, 20, 1
- Conway, J.E., 1996, *Extragalactic radio sources: proceedings of the 175th Symposium of the International Astronomical Union, held in Bologna, Italy, 10-14 October 1995*. Edited by Ron D. Ekers, C. Fanti, and L. Padrielli. Published by Kluwer Academic Publishers, p. 92.
- De Juan, L., Colina, L., Golombek, D., 1996, *A&A*, 305, 776
- De Koff, S., Baum, S.A., Sparks, W.B., et al., 1996, *ApJS* 107, 621
- de Ruiter, H.R., Parma, P., Fanti, C., Fanti, R., 1990, *A&A*, 227, 351
- Fanti, R., Gioia, I., Lari, C., Ulrich, M.H., 1978, *A&AS*, 34, 341
- Fanti, C., Fanti, R., De Ruiter, H.R., Parma, P., 1987, *A&AS*, 69, 57
- Feretti, L., Fanti, R., Parma, P., et al., 1995, *A&A* 298, 699
- Giovannini, G., Feretti, L., Gregorini, L., Parma, P., 1988, *A&A*, 199, 73,
- Gonzalez-Serrano, J.I., Carballo, R., 2000, *A&AS*, 142, 353
- Gonzalez-Serrano, J.I., Carballo, R., Perez-Fournon I., 1993, *AJ*, 105, 1710
- Impey, C., Gregorini, L., 1993, *AJ* 105, 853
- Jaffe, W., Ford, H.C., Ferrarese, L., Van den Bosch, F., O’Connell, R.W., 1993, *Nat*, 364, 213
- Laing, R.A., Parma, P., de Ruiter, H.R., Fanti, R., 1999, *MNRAS*, 306, 513
- Lauer T.R., Ajhar E. A., Byun Y.-I., et al., 1995, *AJ* 110, 2622
- Martel, A.R., Sparks, W.B., Macchetto, F.D., et al., 1998, *ApJ*, 496, 203
- Martel, A.R., Baum, S.A., Sparks, W.B., et al., 1999, *ApJS* 122, 81
- Massaglia, S., Trussoni, E., Caucino, S., et al., 1996, *A&A* 309, 75
- Morganti, R., Fanti, R., Gioia, I.M., et al., 1988, *A&A* 189, 11
- Morganti, R., Ulrich, M.-H., Tadhunter, C.N., 1992, *MNRAS* 254, 546
- Morganti, R., Parma, P., Capetti, A., et al. 1997, *A&AS* 126, 335
- Nagar, N.M., Wilson, A.S., Mulchaey, J.S., Gallimore, J.F., 1999, *ApJS*, 120, 209
- Osterbrock, D. E., 1960, *ApJ* 132, 325
- Parma, P., Fanti, C., Fanti, R., Morganti, R., De Ruiter, H.R., 1987, *A&A* 181, 244.
- Parma, P., De Ruiter, H.R., Fanti, R., Laing, R., 1994, in “The First Stromlo Symposium: The Physics of Active Galaxies”, eds. G.V. Bicknell, M.A. Dopita, P.J. Quinn, ASP Conf. Series, 54, p. 241
- Raimond, E., Faber, S.M., Gallagher, J.S. III, Knapp, G.R., 1981, *ApJ* 246, 708
- Schilizzi, R.T., Fanti, C., Fanti, R., Parma, P., 1983, *A&A* 126, 412
- Sparks, W.B., Golombek, D., Baum, S.A., et al., 1995, *ApJL*, 450, 55
- Trussoni, E., Massaglia, S., Ferrari, R., et al., 1997, *A&A*, 327, 27
- Urry, C.M., Padovani, P., 1995, *PASP*, 107, 803
- Urry, C.M., Falomo, R., Scarpa, R., et al., 1999, *ApJ*, 512, 88
- van Breugel, W., Miley, G., Heckman, T., Butcher, H., Bridle, A., 1985, *A&A* 143, 292
- van der Marel, R.P., van den Bosch, F.C., 1998, *AJ*, 116, 2220
- Verdoes Kleijn, G.A., Baum, S.A., de Zeeuw, P.T., O’Dea, C.P., 1999, *AJ*, 118, 2592
- Worrall, D.M.; Birkinshaw, M.; Cameron, R.A. 1995, *ApJ* 449, 93

This figure "fig4a.jpg" is available in "jpg" format from:

<http://arxiv.org/ps/astro-ph/0009056v1>

This figure "fig4b.jpg" is available in "jpg" format from:

<http://arxiv.org/ps/astro-ph/0009056v1>

This figure "fig4c.jpg" is available in "jpg" format from:

<http://arxiv.org/ps/astro-ph/0009056v1>

This figure "fig4d.jpg" is available in "jpg" format from:

<http://arxiv.org/ps/astro-ph/0009056v1>

This figure "fig4e.jpg" is available in "jpg" format from:

<http://arxiv.org/ps/astro-ph/0009056v1>

This figure "fig4f.jpg" is available in "jpg" format from:

<http://arxiv.org/ps/astro-ph/0009056v1>

This figure "fig4g.jpg" is available in "jpg" format from:

<http://arxiv.org/ps/astro-ph/0009056v1>